Phased Arrays Pre-treatment Evaluation in Antitumoral Hyperthermia

Piero Tognolatti[1] **and Fernando Bardati**[2]

[1]Department of Industrial and Information Engineering and Economics, University of L'Aquila, Italy
[2]Department of Civil Engineering and Computer Science, University of "Tor Vergata", Rome, Italy

Abstract— There is general consensus that quality of hyperthermia treatment is a key factor for clinical effectiveness. The optimal treatment is defined by efficient tumor heating without patient discomfort by hot spots. Two optimization methods with the constraint on amplifier nominal power are presented. A voxel-based numerical analysis is performed for 8 dipoles on two rings, positioned around a head/neck volume within a distilled-water bolus. The optimization methods are compared on the basis of the maximal absolute power delivered to the target and other previously defined parameters.

1. INTRODUCTION

Antitumoral hyperthermia, i.e., increasing the tumor temperature to 40–45°C using an external heating device, is a very effective radio and chemosensitizer, which significantly improves clinical outcome. A correlation between clinical outcome and thermal dose parameters has been shown. The optimal treatment is defined by efficient tumor heating combined with healthy tissue protection from excessive heating. To improve hyperthermia treatment quality, optimization of SAR or temperature distribution in the tumor by hyperthermia treatment planning (HTP) is considered before or during treatment [1–5]. HTP procedures start with tissue map acquisition, then various heating modalities are explored and compared by solving the appropriate electromagnetic (or ultrasound) problem, depending on the equipment in use. Finally the temperature distribution is found for treatment pre-evaluation. However, due to the more complex thermal characterization of vascularised tissues and organs, temperature increase modeling is generally omitted and the optimum problem is formulated in terms of SAR. As the robustness of electromagnetic solvers has increased importantly over recent years, the presently available systems provide excellent opportunities to perform SAR characterization as a start point for SAR optimization. Radiating systems that are currently used to heat deep seated tumors include phased arrays of elementary radiators (dipole, waveguide or microstrip antennas) for which SAR-optimization based HTP is pursued by amplitude and phase setting [6–10].

Objective functions have been proposed for SAR optimization according to various quality indicators [11]. They include maximum absolute SAR and SAR homogeneity in the target both to be optimized as well as hot spots to be minimized. The power deposited in the tumor as a fraction of the net power supplied by the generators and of that delivered to the patient's body are further indicators. For given array, patient and lesion to be heated, evaluating whether or not the array is able to heat the lesion in accordance with prescribed quality indicators is a somehow different problem a solution of which logically precedes HTP. Only in case of positive answer the search for optimal feed settings will be meaningful. The purpose of this paper is to propose means to exploit in this pre-evaluation. Since the electromagnetic solvers decompose the whole body exposed to radiation (both tumor and healthy tissues) into elementary cells, it is natural to treat each cell as a target and to evaluate the maximum SAR deliverable by the array to that cell [12]. At this stage it is sufficient to know that a feed setting exists that is able to deliver such a maximum SAR to that cell. Repeating this for all body cells provides maps of *heatability* that can be used to investigate maximum SAR and SAR uniformity, if the cells belong to a tumor, or to delineate hot spots. Since power deposition is limited by the largest available power from amplifiers referred to as *nominal power*, the latter is included in the optimization problem.

The paper is organized as follows. A voxel-based numerical analysis is performed for an array of 8 antennas on two rings, positioned around a head/neck volume within a distilled-water bolus (Fig. 1). The antennas are half-wave dipole backed by a rectangular metallic reflector [13]. The head/neck numerical phantom is provided by the code used for electromagnetic computations. The code performs a tissue segmentation into $2.08 \times 2.08 \times 2.00\,\mathrm{mm}^3$ cells to which the dielectric parameters are allocated basing on an internal data base. Then the electric field is exported at the nodes of a 3D grid whose side is $\delta = 2\,\mathrm{mm}$. A voxel target is a cube having side δ and centered at a node. Two optimization methods with the constraint on amplifier nominal power are presented. Maps of the power delivered to the voxels are provided. Hot spot generation is a treatment limiting factor. A voxel-based analysis of the hot spots generated by either optimization is presented. Finally the array effect is estimated by an array factor. An extended target (a 60 milliliters sphere) variously centered in the head/neck phantom is considered. The spheres include a large number of voxels allowing for statistical considerations.

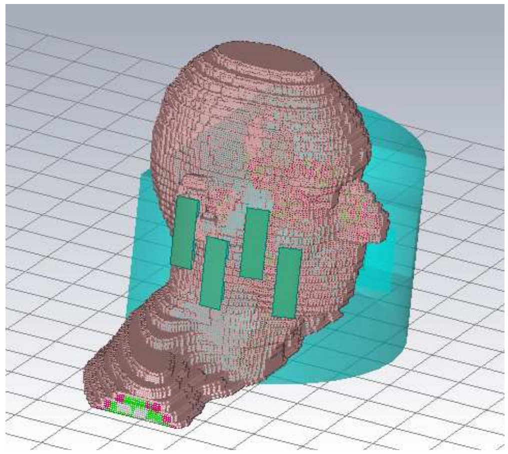

Figure 1: Array of 8 dipoles on 2 rings around a head/neck phantom.

2. POWER-TO-TARGET OPTIMIZATION

An array of M antennas is given that are fed by as much adjustable amplifiers. Let a_n be the complex amplitude of the output wave from the nth amplifier, for $n = 1, \ldots, M$. The power delivered to a target is

$$P = [a]^{T*}[Q][a] \tag{1}$$

where $[Q]$ is the target's $M \times M$ interaction matrix [14]. The vector $[a]$ has entries $a_n = V_n e^{j\varphi_n}$. Amplitudes V_n and phases φ_n are free parameters at operator's disposal for optimization. Hereafter P will be a function of the $2M$ independent variables that are the entries of $[\varphi]$, $[V]$:

$$P = \sum_{m,n=1}^{M} |Q_{mn}|\, V_m V_n e^{j(\psi_{mn} - \varphi_m + \varphi_n)}$$

for $Q_{mn} = |Q_{mn}|\, e^{j\psi_{mn}}$. We assume that the available power of each generator is constrained to be not larger than P_N, i.e.,

$$a_n^* a_n = V_n^2 \leq P_N \tag{2}$$

for any n. An asterisk denotes the conjugate. P_N is amplifier nominal power. We search for a stationary point of P for a_n in the disk $D: V_n \leq \sqrt{P_N}$ on the complex plane.

Posing $\alpha_{mn} = \psi_{mn} - \varphi_m + \varphi_n$, and zeroing the first derivatives with respect to φ_n, V_n we get the system

$$|Q_{k1}| \sin\alpha_{k1} V_1 + |Q_{k2}| \sin\alpha_{k2} V_2 + \ldots + |Q_{kM}| \sin\alpha_{kM} V_M = 0 \quad k = 1, \ldots, M \tag{3}$$

$$|Q_{k1}| \cos\alpha_{k1} V_1 + |Q_{k2}| \cos\alpha_{k2} V_2 + \ldots + |Q_{kM}| \cos\alpha_{kM} V_M = 0 \quad k = 1, \ldots M \tag{4}$$

which can be written as

$$[A][V] = 0$$

$[A]$ is a $2M \times M$ real matrix. Pre-multiplying by $[A]^T$ and posing $[C] = [A]^T [A]$ we obtain

$$[C][V] = 0 \tag{5}$$

i.e. a system of M equations whose M unknowns are the amplitudes V_n. It has solutions which differ from the trivial one, i.e. $[V] = 0$, only if $det[C] = 0$. The interaction matrix of an extended target is positive definite. Consequently, also $[C]$ is positive definite and, therefore, its determinant does not vanish. This result excludes stationary points of P within the disk D. Extremal values of P can be found on the boundary of D, i.e., for $V_n = \sqrt{P_N}$, for any n. The phases φ_n for such extrema are zeroes of

$$\sum_{n=1}^{M} |Q_{kn}| \sin \alpha_{kn} = 0 \quad k = 1, \ldots, M \tag{6}$$

A phase is arbitrary. They can be found by a least square procedure. We name Saturated Amplifier (SA) optimization the procedure which makes this choice for the array phases. Accordingly P^{SA} denotes the power-to-target following SA optimization. P^{SA} is the largest power that an array constrained as shown by (2) can deliver to a target.

A different approach maximizes the ratio $\eta = P/P_G$ where $P_G = [a]^{T*}[a]$ is the power the amplifiers supply to matched loads after amplitude and phase adjustments. η is referred as heating efficiency and depends on $[a]$. Its maximum is the largest eigenvalue λ of $[Q]$ and is obtained for $[a] = [a_{opt}]$ where $[a_{opt}]$ is an eigenvector of $[Q]$ associated to λ. This procedure provides $[\varphi]$ and $[V]$. A phase is arbitrary and the amplitudes are determined except for a scale factor s. In order to find s, the following reasoning applies. The nth generator contributes with $|a_{opt,n}|^2 = V_{opt,n}^2$ to P_G and with $\lambda V_{opt,n}^2$ to P. The best contributing (BC) generator supplies the largest $V_{opt,n}^2$, i.e., $V_{opt,BC}^2$. The equation $s^2 V_{opt,BC}^2 = V_N^2$ provides s. We name Linear Algebra (LA) optimization this procedure. Accordingly

$$P^{LA} = \lambda V_N^2 / V_{opt,BC}^2 P_o \tag{7}$$

is the maximal power that an array constrained by (2) can deliver to a target following LA optimization. In Equation (7), $P_o = 1W$ appears for correct dimensions.

The electromagnetic field was computed by a commercial solver (CST Microwave Studio$^{\mathrm{TM}}$) for a box that includestissues, bolus and air for $102 \times 121 \times 76$ overall nodes. MATLAB$^{\mathrm{TM}}$ was used for the following numerical manipulations. We repeated the optimizations procedures for each voxel belonging to the intersection of the box with the head/neck phantom, denoted Ω hereafter. P_k^{SA} and P_k^{LA} denote the power released to the kth voxel by either optimization, respectively. Color

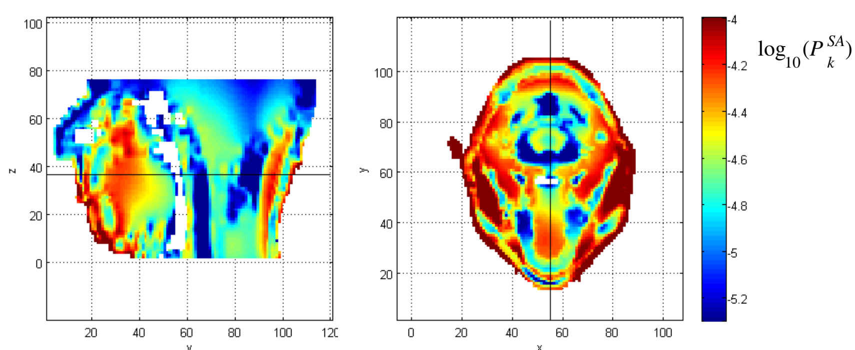

(a)

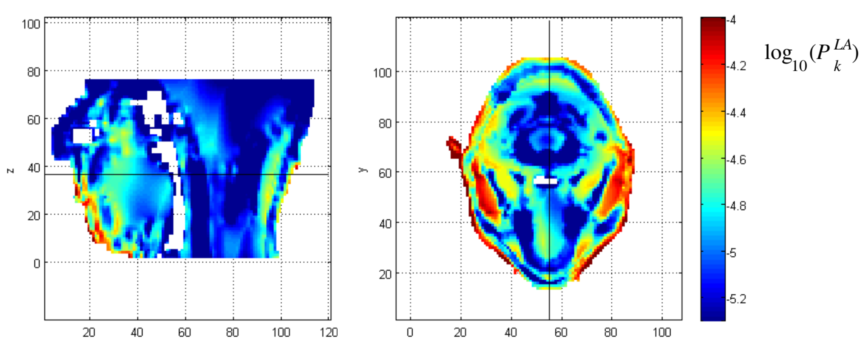

(b)

Figure 2: (a) P_k^{SA} on principal planes (shown by a black bold line) on a logarithmic scale. (b) P_k^{LA} on principal planes.

maps of P_k^{SA} and P_k^{LA} on principal planes passing for the head center are diagrammed in Fig. 2. A logarithmic scale is used to smooth their spread over the treated volume. Due to a larger distance from the dipoles, the voxels that can be less heated are mainly located in the upper head. Due to low values of conductivity σ, they can also be found in spine, trachea, maxillary bones/teeth, and air ducts. A direct comparison shows that P_k^{SA} is 2–3 times P_k^{LA} in most voxels. This advantage is only partially counterbalanced by a decrease of heating efficiency.

3. HOT SPOTS

Hot spots are treatment limiting factors. A discussion on hot spot delineation following phase-amplitude optimization is not a purpose of this paper. Following Wiersma et al. [12], a voxel belongs to a hot spot if the power delivered to it overtakes n times the power to the voxel target. The volumes of such voxels for $n = 1$ and $n = 3$ will be further parameters for comparisons of different heating modalities. Results on hot spot volume (HSV) following SA and LA optimizations and $n = 3$ are presented in Fig. 3. Hot spot volumes of voxels close to the body surface (distance < 1 cm) have not been included in HSV in the assumption that they are well managed by surface cooling. Large HS volumes are found for the voxels shown in Fig. 2 that are more difficult to heat. HS volumes are slightly larger for SAO.

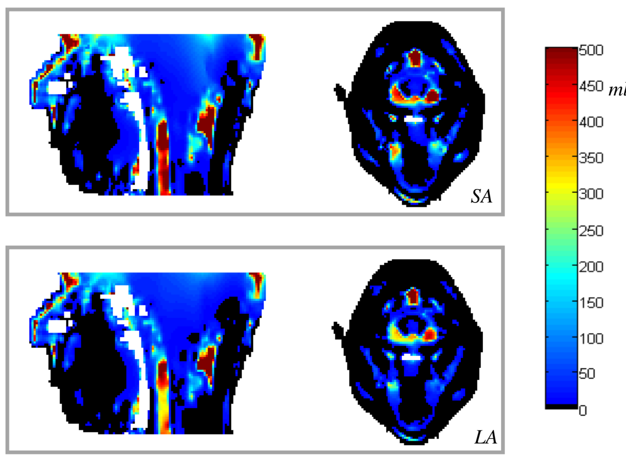

Figure 3: Hot Spot Volume defined in the text for $n = 3$ on principal planes. Each voxel is colored in accordance with HSV when the phased array setting is optimized for the heating of that voxel.

4. ARRAY FACTOR

An array factor AF has been proposed [14] as a figure-of-merit for hyperthermia arrays. AF is defined as the following quotient of heating efficiencies

$$AF = \eta/\eta^\dagger \tag{8}$$

where $\eta^\dagger$ is heating efficiency of the one-element array, i.e., the BP one. The power delivered to the target by a phased array can be equally delivered by the BP channel alone if, however, its power is raised to AF times the power P_G of the array. Since hyperthermia treatments are limited by healthy tissue overheating, the risk is reduced by a M-element phased array as much as $AF \to M$.

Substitution of the heating efficiencies gives the array factor for LA optimization

$$AF^{LA} = \lambda/Q_{BP,BP} \tag{9}$$

It can be shown that $AF^{LA} < M$. $[Q]$ off-diagonal entries are responsible for large values of λ and AF^{LA}. The field interference is more effective as much as the off-diagonal entries comply with $Q_{mn}Q_{nm} \to Q_{mm}Q_{nn}$ [14].

For SA optimization

$$AF^{SA} = P_k^{SA}/(MQ_{BP,BP}) \tag{10}$$

Color plots of AF^{SA} and AF^{LA} are presented in Figs. 4, 5.

A voxel-based analysis precedes overall heatability investigation for an extended target. We considered $60\,\mathrm{cm}^3$ spherical targets with centers differently located in the head/neck segment. The spheres are strongly inhomogeneous in their dielectric properties. The number of voxels within a sphere is large allowing some statistics. The array factor takes values between 0 for SAO (1 for LAO) and $M = 8$. In Fig. 6 AF histograms are shown for the sphere centered at (55, 70, 45), similar results being obtained for other spheres. An interpolation shows that the AF distribution over the sphere voxels is well interpolated by a Weibull 3-parameter distribution. The shape parameter is 2.34 for LAO and 2.20 for SAO, being slightly greater than 2, which is the case of a Rayleigh distribution. These results are preliminary showing however that the head/neck region being highly dielectrically inhomogeneous, predictive wave-based propagation models may be inaccurate.

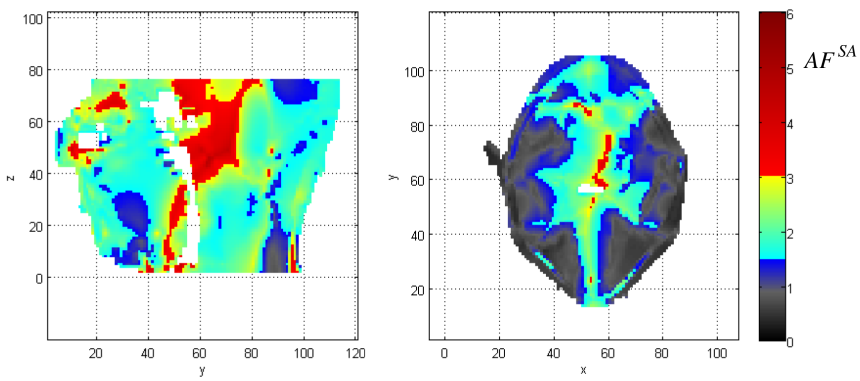

Figure 4: Arrayfactor AF^{SA} on the principal planes. Zones of low and high AF^{SA} are well distinguishable. The zone where $AF^{SA} \leq 1$ is shown in grayscale. White pixels are air filled.

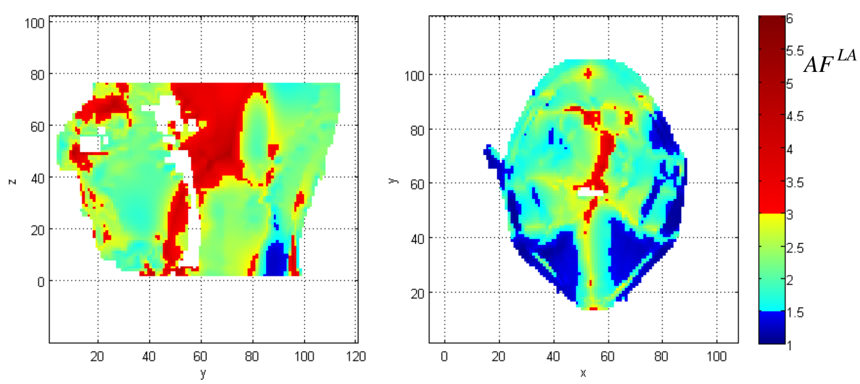

Figure 5: Array factor AF^{LA} on the principal planes.

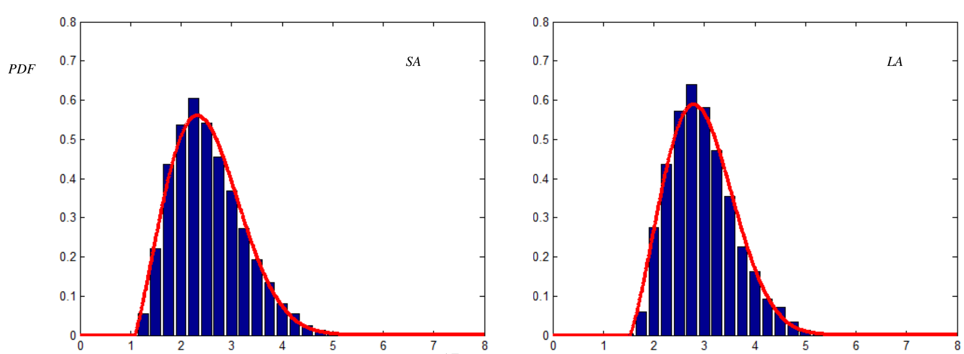

(a) (b)

Figure 6: Histograms of AF for the voxels belonging to the sphere. (a) SA optimization, and (b) LA optimization. Interpolating Weibull probability density functions also shown (red curves).

5. CONCLUSION

Phased arrays are currently exploited in antitumoral microwave hyperthermia. For given array, patient and tumor to be heated, evaluating whether the array is able to heat the tumor in accordance with prescribed quality indicators logically precedes amplitude and phase setting for treatment planning. This paper proposes some means to exploit in this pre-evaluation. The optimal treatment is defined by efficient tumor heating without patient discomfort by hot spots. Two optimization methods with a constraint on the maximal available power from the set of amplifiers have been introduced. A voxel-based numerical analysis was performed for 8 dipoles on two rings, positioned around a head/neck volume within a distilled-water bolus. The results of the optimizations have been compared on the basis of the maximal absolute power delivered to the target, hot spot volumes and other parameters. An extended target like a tumor includes many voxels allowing for some statistics. Preliminary results for a large and highly inhomogeneous spherical target have been presented.

REFERENCES

1. Gellermann, J., P. Wust, D. Stalling, M. Seebass, J. Nadobny, R. Beck, H. Hege, P. Deuflhard, and R. Felix, "Clinical evaluation and verification of the hyperthermia treatment planning system hyperplan," *Int. J. Radiat. Oncol. Biol. Phys.*, Vol. 47, 1145–1156, 2000.
2. Sreenivasa, G., J. Gellermann, B. Rau, J. Nadobny, P. Schlag, P. Deuflhard, R. Felix, and P. Wust, "Clinical use of the hyperthermia treatment planning system HyperPlan to predict effectiveness and toxicity," *Int. J. Radiat. Oncol. Biol. Phys.*, Vol. 55, 407–419, 2003.
3. Van Haaren, P. M. A., H. P. KoThk, C. A. T. Van den Berg, Z. V. S. V. PJ, S. Oldenborg, L. J. Stalpers, M. S. Schilthuis, A. A. C. De Leeuw, and J. Crezee, "On verification of hyperthermia treatment planning for cervical carcinoma patients," *Int. J. Hyperthermia*, Vol. 23, 303–314, 2007.
4. Franckena, M., R. Canters, F. Termorshuizen, J. Van der Zee, and G. C. Van Rhoon, "Clinical implementation of hyperthermia treatment planning guided steering: A cross over trial to assess its current contribution to treatment quality," *Int. J. Hyperthermia*, Vol. 26, 145–157, 2010.
5. Kok, H. P., S. Ciampa, R. De Kroon-Oldenhof, E J. Steggerda-Carvalho, G. Van Stam, P. J. Zum Vörde Sive Vörding, L. J. A. Stalpers, E. D. Geijsen, F. Bardati, A. Bel, and J. Crezee, "Toward on-line adaptive hyperthermia treatment planning: Correlation between measured and simulated specific absorption rate changes caused by phase steering in patients," *Int. J. Radiat. Oncol. Biol. Phys.*, Vol. 90, 438–445, 2014.
6. Turner, P. F. and T. Shaefermeyer, "BSD-2000 approach for deep local and regional hyperthermia: Clinical utility," *Stahlenther Onkol.*, Vol. 165, 700–704, 1989.
7. Van Dijk, J. D., C. Schmeider, R. van Os, L. E. Blank, and D. G. Gonzales, "Results of deep body hyperthermia with large waveguide radiators," *Adv. Exp. Med. Biol.*, Vol. 267, 315–319, 1990.
8. Crezee, J., H. P. Kok, J. Wiersma, G. van Stam, J. Sijbrands, A. Bel, et al., "Improving locoregional hyperthermia equipment using 3-D power control: From AMC-4 to AMC-8," *Graz: Proc 22nd Annual Meeting of ESHO*, Vol. 14–15, 2005.
9. Nadobny, J., W. Wlodarczyk, L. Westhoff, and J. Gellermann, "Development and evaluation of a three-dimensional hyperthermia applicator with water-coated antennas (WACOA)," *Med. Phys.*, Vol. 30, 2052–2064, 2003.
10. Paulides, M. M., J. F. Bakker, E. Neufeld, J. van der Zee, P. P. Jansen, P. C. Levendag, et al., "The HYPERcollar: A novel applicator for hyperthermia in the head and neck," *Int. J. Hyperthermia*, Vol. 23, No. 7, 567–576, 2007.
11. Canters, R. A. M., P. Wust, J. F. Bakker, and G. C. Van Rhoon, "A literature survey on indicators for characterisation and optimisation of SAR distributions in deep hyperthermia, a plea for standardization," *Int. J. Hyperthermia*, Vol. 25, No. 7, 593–608, 2009.
12. Wiersma, J., N. Van Wieringen, H. Crezee, and J. D. P. Van Dijk, "Delineation of potential hot spots for hyperthermia treatment planning optimisation," *Int. J. Hyperthermia*, Vol. 23, No. 3, 287–301, 2007.
13. Bardati, F. and P. Tognolatti, "A voxel-based approach in phased-array optimization for microwave hyperthermia," *44th European Microwave Conference (EuMC)*, 786–789, IEEE, 2014.
14. Bardati, F. and P. Tognolatti, "Figures of merit and their bounds in radiofrequency heating by phased arrays," *Int. J. Hyperthermia*, Vol. 23, No. 7, 567–576, 2013.